LIMNOLOGY
and
OCEANOGRAPHY: METHODS

ASLO

Limnol. Oceanogr.: Methods 2021

doi: 10.1002/lom3.10416

Measuring pH in low ionic strength glacial meltwaters using ion selective field effect transistor (ISFET) technology

Elizabeth A. Bagshaw,[1]* **Jemma L. Wadham**,[2] **Martyn Tranter**,[2] **Alexander D. Beaton**,[3] **Jon R. Hawkings**,[2,4,5] **Guillaume Lamarche-Gagnon**,[2] **Matthew C. Mowlem**[3]

[1]School of Earth and Ocean Sciences, Cardiff University, Cardiff, UK
[2]School of Geographical Sciences, University of Bristol, Bristol, UK
[3]National Oceanography Centre, Southampton, UK
[4]Department of Earth, Ocean and Atmospheric Science, Florida State University, Tallahassee, Florida
[5]German Research Centre for Geosciences GFZ, Potsdam, Germany

Abstract

Measuring pH in glacial meltwaters is challenging, because they are cold, remote, subject to freeze-thaw cycles and have low ionic strength. Traditional methods often perform poorly there; glass electrodes have high drift and long response times, and spectrophotometric techniques are unpractical in cold, remote environments. Ion selective field effect transistor (ISFET) sensors are a promising alternative, proven in marine and industrial applications. We assess the suitability of two models of ISFET, the Honeywell Durafet and Campbell Scientific Sentron, for use in glacial melt through a series of lab and field experiments. The sensors have excellent tolerance of freeze-thaw and minimal long-term drift, with the Durafet experiencing less drift than the Sentron model. They have predictable response to temperature, although the Durafet housing causes some lag during rapid cycling, and the impact of stirring is an order of magnitude less than that of glass electrodes. At low ionic strength (< 1 mmol L^{-1}), there is measurable error, but this is quantifiable, and less than glass electrodes. Field tests demonstrated low battery consumption, excellent longevity and resistance to extreme conditions, and revealed biogeochemical processes that were unlikely to be recorded by standard methods. Meltwater pH in two glacial catchments in Greenland remained > 7 with consistent diurnal cycles from the very first meltwater flows. We recommend that ISFET sensors are used to assess the pH of glacial meltwater, since their tolerance is significantly better than alternative methods: the Durafet is accurate to ± 0.2 pH when waters are > 1 mmol L^{-1} ionic strength, and ± 0.3 pH at < 1 mmol L^{-1}.

Meltwater from the Greenland ice sheet and other land ice in the Arctic is contributing approximately 600 km^3 yr^{-1} to the oceans (Bamber et al. 2018). The chemical composition of these waters has the potential to significantly influence the oceans, by changing carbon and nutrient budgets (Hood et al. 2009, 2015; Hawkings et al. 2015; Hopwood et al. 2020; Kellerman et al. 2020), influencing marine food webs (Arrigo et al. 2017; Hopwood et al. 2018) and potentially controlling CO_2 dynamics (Fransson et al. 2015; Beaird et al. 2018; St. Pierre et al. 2019). The nature of glacial meltwaters means that they are challenging to monitor, because of low temperatures, low ionic strength, rapidly changing discharge, and high turbidity and sedimentation. Despite these challenges, it is critical to understand their chemistry so that the impact of increasing meltwater flux can be predicted. Various studies have measured chemical and biogeochemical parameters in meltwater (e.g., *see* Wadham et al. 2019), but few have presented consistent, accurate, high-resolution measurements of pH over meaningful timescales.

Accurate measurement of pH is a critical component of biogeochemical monitoring schemes, crucial for understanding the impact of glacial meltwaters downstream (Tranter 2003; Hawkings et al. 2015; Raiswell et al. 2018; Wadham et al. 2019) and potential for CO_2 drawdown. pH is a "master variable" for determining the chemical characteristics of aqueous solutions since it exerts a first order control on the speciation and solubility of many entities, including dissolved inorganic C, P, Fe, Al, and Si species and the partial pressure of CO_2 in solution. In the field, it is typically measured via potentiometric glass electrodes, or by spectrophotometric analysis. Spectrophotometric methods have been used in marine and freshwater systems to obtain extremely accurate

*Correspondence: bagshawe@cardiff.ac.uk

Additional Supporting Information may be found in the online version of this article.

measurements of pH and are generally insensitive to ionic strength (Clayton and Byrne 1993). However, methods are generally complex, incompatible with high turbidity, freezing, and limited to the range of the chosen indicator (Liu et al. 2011).

Potentiometric electrodes offer the convenience and instant analysis desired for field applications, but are not always suited to long-term monitoring of meltwater systems. They are compromised by low temperatures, frequent freeze-thaw, high concentrations of suspended sediment, and low ionic strength. Ionic strength of glacier melt typically ranges from 10^{-4} to 10^{-3} mol L^{-1} and suspended sediment from 1 to 10 g L^{-1} (Cowton et al. 2012). pH is typically 6–9 (Hawkings et al. 2015), although some early season meltwaters and supraglacial ecosystems may range from 4 to 10 (Tranter et al. 2004). Low ionic strength waters have a low potential supply of electrons to the measuring electrode (Bates 1973), which can significantly impact the performance. Even at higher ionic strength, glass electrodes are subject to drift of up to 0.02 pH d^{-1} (Rerolle et al. 2012), which worsens when ionic strength is $\leq 10^{-3}$ mol L^{-1} (Covington et al. 1983; Davison and Woof 1985). Meltwaters are often out of equilibrium with atmospheric CO_2 when they emerge from beneath the ice (St. Pierre et al. 2019), so rapid measurement of pH is crucial for accurate assessment of their partial pressure of CO_2 (Metcalf 1984). This is difficult with the slow response times of glass electrodes in meltwaters (Ryu and Jacobson 2012). In cases of best practice, use of low ionic strength buffers and frequent recalibration of the glass electrode sensor can generate usable data, but long-term data sets from glacier melt are frequently compromised by excessive drift and long electrode response times.

An alternative measurement method is an ion selective field effect transistor (ISFET). ISFET sensors have been the subject of extensive investigation over the past two decades (Bergveld 2003), and ISFETs for pH measurement are commercially available from a number of suppliers (Honeywell, Campbell Scientific, Microsens, Mettler Toledo, Hach Lange). These sensors perform over a wide range of the pH scale, and are typically robust and easy to use (Martz et al. 2010). They have been successfully deployed in a range of industrial systems and natural waters, including low temperature marine waters beneath sea ice (Matson et al. 2011, 2014) as well as coastal waters (McLaughlin et al. 2017) and the deep sea (Johnson et al. 2016). Previous studies demonstrated that ISFETs produce a 100% Nernstian response, with stable and repeatable potential at constant temperature, salinity, and pH (Bresnahan Jr et al. 2014; Takeshita et al. 2014) and that they exhibit exceptional stability over long-term deployments in seawater (Martz et al. 2010; Bresnahan Jr et al. 2014). ISFET sensors have very low impedance, hence much more rapid response and lower drift than a potentiometric electrode. However, no data exist on their performance in cold, low ionic strength waters, and manufacturers generally caution against use at very low ionic strengths (< 10 μS cm^{-1} [c. 0.16 mmol L^{-1}], Honeywell Durafet). Given their performance in field studies in other aquatic systems, they are nevertheless the most promising technology for assessing the pH of glacial meltwater. Before they can be used with confidence, the potential sources of error associated with their performance in low ionic strength systems, which also are subject to freeze-thaw cycles and high flows, must be quantified. This study aims to assess the performance of two commercially available examples of ISFET sensors for determining pH in glacial meltwaters, and use them to reveal high resolution cycling in glacial meltwater river pH hitherto unseen in the early season melt from the Greenland ice sheet.

Materials and procedures

Laboratory tests

We conducted a series of laboratory experiments to evaluate the performance of ISFET sensors in low ionic strength waters, simulating three key aspects of the aqueous glacial environment: low temperatures, freeze-thaw, and varying flow rates. The lab-tested sensors were then field deployed in glacial meltwater rivers draining the south and southwest of the Greenland Ice Sheet, and a valley glacier in Svalbard.

Two models were tested, the Honeywell Durafet (Models II and III), and the Sentron ISFET, supplied by Campbell Scientific (CS526). The Durafet electrodes were used with a Honeywell DL421 sensor module, which transmits a temperature compensated current loop proportional to the pH sensed by the electrode. Both sensors were controlled by a Campbell Scientific CR1000 datalogger. The Durafet sensor required additional (bespoke) circuitry to convert the current output to a voltage which could be recorded by the datalogger. The Durafet Models II and III are similar, although the Model III is fully waterproof with an entirely submersible sensor head. Laboratory tests were generally performed on the Model II, where the sensor tip alone could be submerged, but field deployments were undertaken on the Model III. We used the in-built Ag/AgCl reference electrode of both sensors, and designed the evaluations to mimic field conditions as closely as possible. The raw mV response of the ISFET sensors was recorded by the datalogger throughout all tests. When required, this was related to a pH value using a two point linear calibration using commercially available low ionic strength buffers (Camlab) at the experimental temperature, performed before and after the experiments, and occasionally during.

Temperature, freeze-thaw, drift, and response time

The impact of low temperatures and freeze-thaw processes was simulated in temperature controlled incubators (LMS, UK), with independent temperature sensors (Campbell Scientific 107). Temperature was repeatedly cycled between −10°C and +15°C, and −5°C and +15°C while the electrodes were immersed in 2 mmol L^{-1} $NaHCO_3$. Electrode response was measured during both up- and downcycling.

To assess drift, sensors were installed in the same 2 mmol L^{-1} $NaHCO_3$ solution for 60 d at 1–3°C, with electrode response measured every 30 s. The drift at varying ionic strength was assessed by repeating the experiment with commercial buffer solutions, classified as low (Camlab), medium (Sigma), and high (Fisher) ionic strength. The response time was tested at 3°C and 1.5°C. Mean t90, the time taken for 90% of the signal change to occur, was assessed by measuring electrode response every second when moving between high (6.96) and low (4.01) low ionic strength buffer solutions.

Stirring

Variations in the flow rate of the solution being measured can cause "streaming effects" which result in erroneous pH measurements. This streaming potential is caused by disturbance of charge density on the electrode surface (Bates 1973), and for accurate measurements an undisturbed solution is recommended. This is rarely possible in environmental systems, so we assessed the possible impact of stirring on pH measurements. Glacial meltwaters are typically turbid (usually ~ 1 g L^{-1} but up to 13 g L^{-1}, Knudsen et al. 2007) and fast flowing (up to 60 m s^{-1}; Beaton et al. 2017), making them challenging to mimic in the laboratory (Fig. 1). Turbidity should have no impact on the ISFET chip operation if the sensor head is not fouled, but to assess the impact of flow (and hence streaming potential at the electrode head), sensors were installed in buffer solutions of pH 4.01, 6.96 (Camlab), and 9.11 (custom $NaHCO_3$), agitated at either 0, 0.02, or 0.2 m s^{-1} with a large magnetic stirrer. These are well below the water velocities measured in the field, but were a reasonable first-order investigation of the existence of streaming effects.

Ionic strength

There are several commercially available low ionic strength buffer solutions, but these are only available in limited pH ranges (4.10 and 6.96 [Camlab, UK]; 4.75, 6.97, and 9.15 [Thermo Orion]). Additionally, the high pH solution has a short shelf-life, and the ionic strengths are generally in excess of many glacial meltwaters (5 mmol L^{-1} vs. 0.2–5 mmol L^{-1}). These commercial buffer solutions were used for calibration and periodic sensor drift tests during field deployments, but to test the impacts of ionic strength and long-term drift on sensor performance, custom buffers of extremely low ionic strength were made up using deionized water and $NaHCO_3$, ranging from 0.7 to 40 mmol L^{-1}. Solutions were allowed to air equilibrate at the test temperature (3°C) and then capped with a gas tight rubber stopper into which the pH probes were implanted. Aliquots of each experimental solution were syringed from the vessel and sealed in water-full, gas tight vials, kept at the experimental temperature in Weiss low temperature cabinets (± 0.2°C) until analysis. The pH probes remained in each solution for between 20 min and 4 h, with mV output and solution temperature recorded every second by the CR1000 datalogger. The mean mV over 2 min at the time of sampling was converted to pH via two point calibration in low ionic strength buffer solutions (Camlab, as above) at the experimental temperature.

The theoretical pH of the air-equilibrated solution was modeled using the USGS water speciation program PhreeqQC, and the pH confirmed using standard spectrophotometric methods (Clayton and Byrne 1993; Dickson et al. 2007). All spectrophotometric measurements were conducted on a Cary 60 UV-Vis spectrophotometer, using *m* Cresol purple (mCP)

Fig 1. Sediment-rich, fast-flowing, turbid meltwaters in the Qinnguata Kuussua (Watson River), Kangerlussuaq, Greenland, a typical large glacial outflow.

indicator sodium salt (Sigma Aldrich, pH range 7.4–9, pKa = 8.32). The indicator was purified (Liu et al. 2011) via flash chromatography (Patsavas et al. 2013) using a RediSep Rf Gold C18 column (Teledyne), and the extinction coefficient for each sample run was calculated by measuring absorbance at wavelengths of the isobestic, nonabsorbing, and the absorption maxima of acid and base forms of the indicator (434, 488, 578, and 730 nm wavelengths) (Clayton and Byrne 1993). Analysis occurred within 5 h, in new disposable 10 mm pathlength cuvettes at the experimental temperature, which was verified by an external probe. Absorbance was converted to pH using standard methods (Dickson et al. 2007), with pK_I calculated at our experimental temperatures using published temperature dependence for mCP (Lai et al. 2017).

Field tests

The sensors were tested in glacial meltwaters at Kiattut Sermiat, S Greenland (61.2°N, 45.3°W), Leverett Glacier, SW Greenland (67.06°N, 50.17°W), and Bogerbreen, Spitsbergen, Svalbard (78.2°N, 15.6°E). The Durafet III was deployed for 2.5 months in a shallow proglacial meltwater stream at Kiattut Sermiat (maximum discharge = 57 m^3 s^{-1}, maximum suspended sediment = 0.22 g L^{-1}) in summer 2013, and for 1 month in a larger meltwater stream at Leverett Glacier in early spring 2015 (maximum spring [May] discharge = 150 m^3 s^{-1}, Hawkings et al. 2015; and suspended sediment = 5 g L^{-1}, Cowton et al. 2012). Mean air temperature during the deployment at Kiattut Sermiat was 7.4°C, ranging from −5.4°C to 19.8°C, and 1.9°C at Leverett Glacier, ranging from −3.2°C to 8.6°C. The Sentron probe was deployed for 2 weeks in a turbid meltwater stream exiting Bogerbreen in Endalen, Svalbard in August 2015. Mean air temperature was 5.9°C, ranging from 1.9°C to 20.9°C, and suspended sediment ranged from 2 to 6 g L^{-1}.

The Durafet sensors were controlled by Campbell Scientific CR1000 dataloggers, and the Sentron by a CR10X, which triggered sensor readings every 30 s and logged an average every 15 min. Electrical conductivity (EC, used as a proxy for total dissolved solids and hence an indicator of ionic strength) and water temperature were monitored alongside pH by a Campbell Scientific 247 probe. Drift tests of the pH probes (immersion of the sensor head in low ionic strength pH 6.96 buffer solution for 5–15 min) were conducted weekly with the mV and temperature reading noted, and manual readings were taken using Beckman 500 series glass electrodes, calibrated daily with low ionic strength buffers. Sensors remained in situ throughout the tests, powered by lead-acid batteries trickle-charged by solar panels.

Assessment

Laboratory tests: Drift, response time, and temperature

Long-term drift tests confirmed results reported by numerous authors (Martz et al. 2010; Hofmann et al. 2011; Matson et al. 2011; Gonski et al. 2017; McLaughlin et al. 2017), which demonstrate drift in pH of < 0.1 over deployments of weeks to months. The maximum drift in pH observed over the 60 d laboratory tests at 2°C was 0.08, and in a 3 month field test in the proglacial stream of Kiattut Sermiat, S Greenland, 0.07. Supporting Information Figure S1 shows detailed drift tests at low temperatures (2°C). Maximum pH drift in low ionic strength solutions was 0.08 in the Durafet, and 0.17 for the Sentron. At high ionic strength, maximum drift was 0.03 for both sensors. Mean response t90 (n = 5), the time taken for 90% of the signal change to occur, was 16 s for the Durafet Model II and 141 s for the Sentron (Supporting Information Fig. S2).

Both sensors survived freeze-thaw testing, retaining performance following repeated temperature cycling between −10°C and +15°C, and −5°C and +15°C, in bespoke low ionic strength $NaHCO_3$ buffers. There was some fluctuation in the signal during the freezing and thawing of solution around the probes (see an example cycle in Supporting Information Fig. S3), but as the ice crystals formed/melted, the reading stabilized and a constant signal was output to the datalogger. The sensors reported pH values up to 0.5 lower when the solution was frozen. This was most likely because either (1) the sensors were not recording the true pH of the solution because the formation of ice crystals impeded the current traveling through the ISFET, or (2) the small quantities of solution remaining in the ice crystal matrix were chemically altered during the freezing process. Both sensors recovered well after freezing, with reported pH returning to near-identical values (± 0.02) to that recorded prior to freezing.

The performance of the Durafet automatic temperature compensation (ATC) over the range of temperatures from −7°C to +12°C was assessed by comparing the mV output of the sensor (with ATC) against the temperature (Fig. 2). This should be corrected by the ATC, but as Fig. 2 shows, there is a significant response to changing temperature in addition to that compensation. Temperature was cycled in both directions, and there was no difference in response. The difference between the manufacturer's ATC and the recorded output is equivalent to 0.02 pH/°C when mV was converted to pH using a standard two-point calibration with low ionic strength buffers (Fig. 2, r^2 = 0.77).

Laboratory tests: Stirring and ionic strength

Flow velocity had a measurable impact on sensor output (Fig. 3). The pH signal changed by up to 0.03 pH units when the solution was stirred. There was no significant difference between the response in low, medium, or high pH buffers, or between the two tested velocities (0.2 vs. 0.02 m s^{-1}).

Figure 4 shows the variance between pH measured by the Durafet and Sentron sensors, calculated by two point calibration with commercial low ionic strength buffers (Camlab), and that determined spectrophotometrically with meta-cresol purple. Both sensors had an offset between measured and predicted pH when ionic strength was < 1 mmol L^{-1}, although

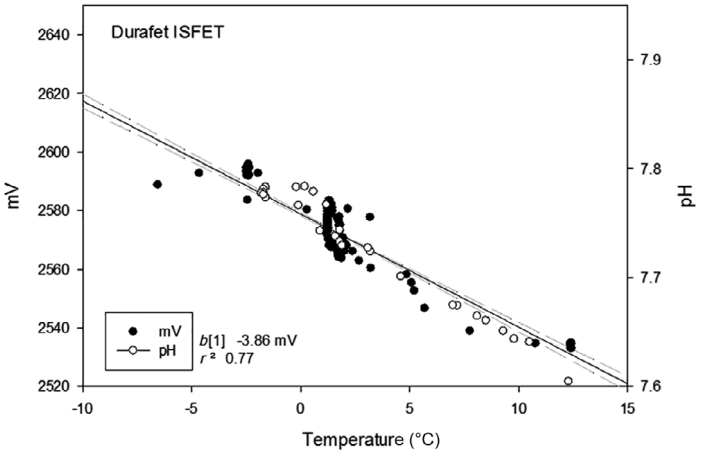

Fig 2. Sensitivity of the Durafet to temperature, beyond the automatic compensation provided by the electrode's built-in temperature sensor. The pH computed from the mV by the calibration with low ionic strength buffers is shown for ease of interpretation.

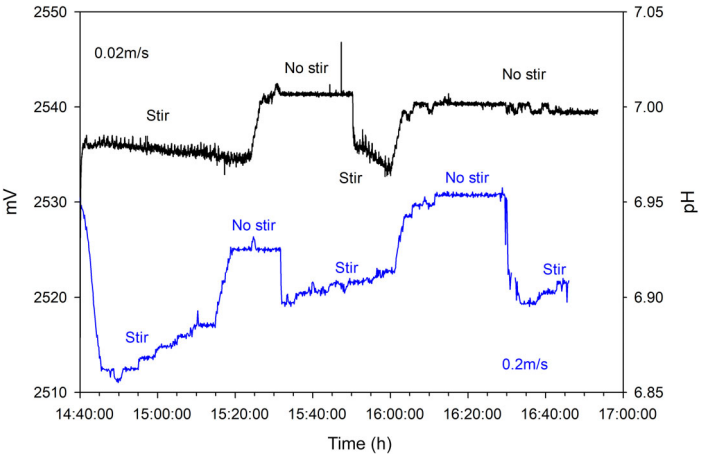

Fig 3. Response of Durafet sensor to varying flow rates in low ionic strength buffer solution (Camlab 6.96). "No stir" indicates that the solution was stationary, whereas "Stir" shows when the solution was agitated at speeds of 0.2 and 0.02 m s^{-1}, as labeled.

these were more significant in the Sentron (up to 0.8 pH) compared with the Durafet (up to 0.2 pH). Across the total ionic strength range, the mean Sentron offset was lower (< 0.05) than the Durafet (< 0.15), but the Durafet performed better in the lowest ionic strength solutions. There was no difference between solutions spiked with NaCl or $MgSO_4$, suggesting that ion size does not significantly impact measurement.

Field tests

The Sentron and Durafet sensors both performed well in field tests in Greenland and Svalbard. Sensors ran continuously while unattended throughout the monitoring periods, powered by solar-charged lead acid batteries with measurements

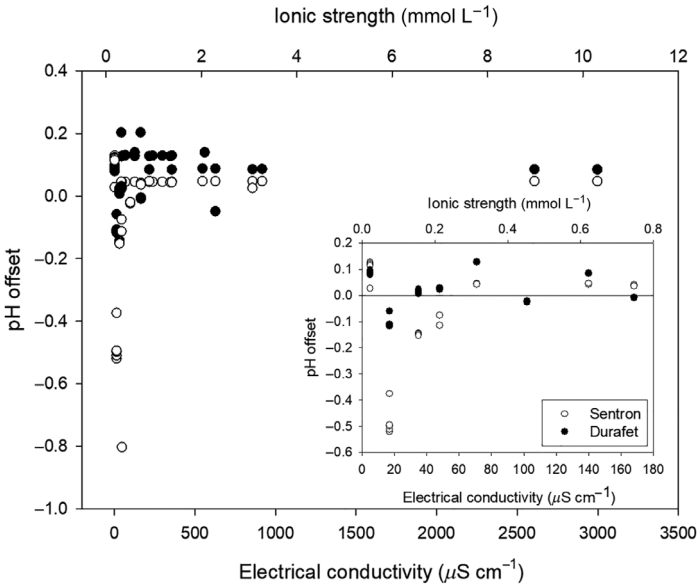

Fig 4. Offset between pH measured by the Durafet and Sentron ISFET sensors and determined spectrophotometrically by meta-cresol purple in solutions of varying ionic strength. Buffers were made up from $NaHCO_3$ spiked with either NaCl or $MgSO_4$, allowed to air equilibrate at 3°C, and capped with gas-tight stoppers through which the probes were inserted. pH was recorded by dataloggers, and samples removed for spectrophotometric analysis via syringe (*see* "Methods" section). There was no difference between the $MgSO_4$ and NaCl spiked buffers. The inset shows the concentration range of most relevance to glacial meltwaters (< 180 µS cm^{-1}).

triggered and recorded by Campbell Scientific dataloggers. Manual readings with handheld potentiometric probes were taken daily at Kiattut Sermiat (Fig. 5B) and sporadically at Leverett Glacier and Bogerbreen (Fig. 5C,D). They showed good agreement with the ISFET sensors, although there were some discrepancies in the early part of the season at Kiatutt Sermiat. We hypothesize that this variance was in part because multiple field personnel operated the probe, whereas later measurements were made consistently by a single operator. This aptly illustrates the difficulty in obtaining glass electrode pH readings in low ionic strength waters that are out of equilibrium with the atmosphere (*see* Ryu and Jacobson 2012 Methods section)—readings can be somewhat subjective, whereas the data reported by the Durafet and Sentron sensors are independent of user interpretation.

At Kiattut Sermiat, the EC ranged from 17 to 47 µS cm^{-1} throughout the deployment, within the range of our low ionic strength laboratory tests and typical of glacial meltwaters across the world (Bagshaw et al. 2016). The maximum pH sensor drift over the complete 2.5 month deployment was 0.07, determined by weekly comparison with commercial low ionic strength buffer solution (Camlab pH 6.96). The Durafet recorded shifts in pH associated with evolution of the subglacial drainage system (Bartholomew et al. 2010; Hatton et al. 2019). The shift to an efficient system, which transports

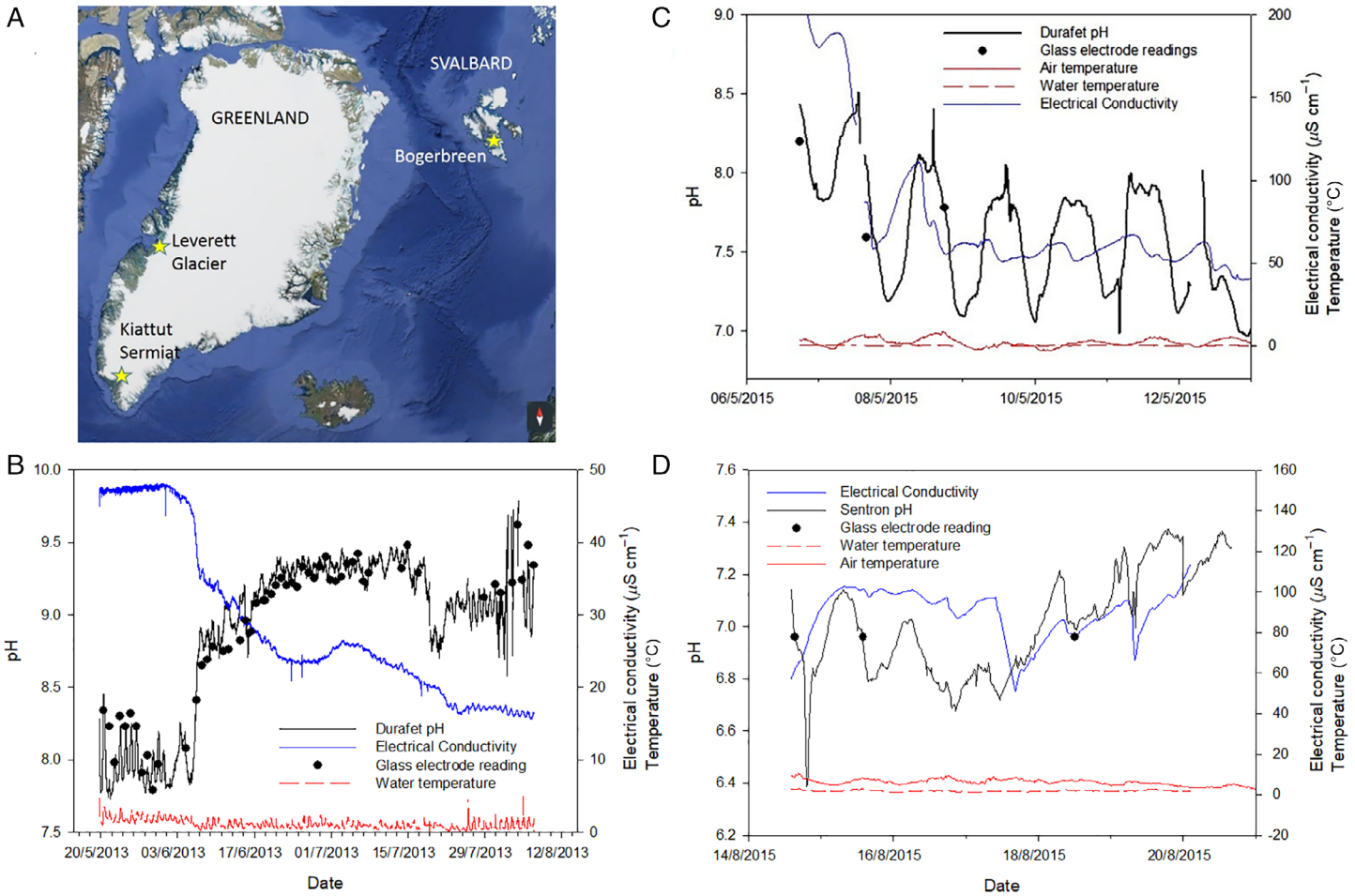

Fig 5. (**A**) Deployment sites of ISFET sensors in proglacial meltstreams across the Arctic at (**B**) Kiattut Sermia and (**C**) Leverett Glacier, S Greenland and (**D**) Endalen, Bogerbreen, Svalbard (note the differing scales). The Leverett Glacier deployment occurred at the very start of the melt season under repeated diurnal freeze-thaw conditions. Base map from Google Earth.

ice melt rapidly to the glacier margin, is indicated by a drop in EC (from ~ 48 to ~ 20 μS cm^{-1}) and a rise in pH (~ 8 to ~ 9) on the June 6th, which show less concentrated water exiting the glacier (Hawkings et al. 2016). The sensors also record a melt pulse observed on June 19th, which lowers pH (from 9.2 to 8.7) with a concurrent decrease in EC (the associated discharge record can be seen in Hawkings et al. 2016).

In the second Greenland deployment at Leverett Glacier, air temperatures were much lower (mean 1.9, minimum −5°C), and waters more concentrated at the very start of the melt season (mean 64, maximum 260 μS cm^{-1}). Sensor drift over the deployment was 0.03. Strong diurnal cycles in the pH and EC records, with daily changes of up to 0.8 pH and 70 μS cm^{-1}, demonstrate the melt and freeze of snow, slush, and surface melt. The sensors survived repeated overnight freezing, and were capable of recording the pH of the slushy margins of the nascent proglacial river. The pH ranged from 7 to 8.5 in this time period, and manual samples were in good agreement with the Durafet record.

The Sentron probe was deployed in Svalbard, and also showed good agreement with the limited manual readings. The sensor recorded diurnal cycles of up to 0.3 pH. The meltwater stream did not freeze during sampling, with air temperature ranging from 1.9°C to 10°C and water temperature from 1.3°C to 3.1°C. EC ranged from 58 to 113 μS cm^{-1}, and pH from 6.4 to 7.4.

Discussion

Glacial meltwaters have a strong influence on downstream environments, including into shelf seas surrounding ice sheets (Hendry et al. 2019). They can impact carbon dynamics (Hood et al. 2015; Wadham et al. 2019) and influence CO_2 systems (Fransson et al. 2015; Graly et al. 2017; St. Pierre et al. 2019), but accurate measurement of meltwater pH is challenging, particularly over long time periods and at high resolution. Sampling regimes to date have relied on regular spot sampling, conducted during the height of the melt season. These data

have been invaluable in discovering how meltwaters behave at peak flow, but are insufficient for understanding how biogeochemical processes operate from melt onset, and for coverage of the full diurnal flow cycle (*see* Fig. 5). Many meltwaters will have been isolated from the atmosphere, which means measurement as soon as possible after they emerge from beneath the ice is paramount (Metcalf 1984), but not always possible. High-frequency measurements can help resolve the temporal and spatial patterns and trends that traditional discrete water sampling is unable to capture (Gonski et al. 2017). However, standard potentiometric electrodes are subject to drift over long deployments, so even automated potentiometric systems require frequent recalibration and maintenance. ISFET sensors can operate for long periods without maintenance, which eliminates many of the problems associated with measuring high resolution pH in the field.

The use of ISFET sensors has been well demonstrated in marine environments (Martz et al. 2010; Bresnahan Jr et al. 2014), including at low temperatures (Matson et al. 2011, 2014; Rérolle et al. 2016), and recently in estuarine waters with varying salinity (Gonski et al. 2017). However, their performance is unproven in low ionic strength freshwaters, including glacial melt. We believe that ISFETs are well suited to glacial deployments since they are small, robust, require low power and are insensitive to turbidity. Other authors have demonstrated that their drift is minimal, even over long deployments (Martz et al. 2010; Hofmann et al. 2011), and our results confirm this, both in the laboratory and the field, and at low temperatures and low ionic strengths. The maximum drift experienced by the Durafet during the 4 week laboratory tests was 0.08, and in the 10 weeks in the field, 0.07. The Sentron drift was more significant, at 0.17, but still better than equivalent glass electrodes. ISFET pH sensors therefore represent a genuine advance in water monitoring technology.

The two versions of ISFET sensors tested (Campbell Scientific Sentron and Honeywell Durafet) were both capable of surviving repeated freeze-thaw cycling, and the Durafet performed effectively during field deployment in an emerging glacial meltwater stream, with slushy margins and overnight freezing in early spring. This supports other literature which demonstrate good performance at low temperatures (Hofmann et al. 2011; Matson et al. 2014), although the sensors did not undergo freeze-thaw cycling during these sea ice deployments, which are characterized by stable, if low, temperatures. However, our tests demonstrate that the Durafet automatic temperature compensation did not perform as expected (Fig. 2). The sensors themselves do exhibit a Nernstian response ($R{\cdot}\ln(10)/F$ = 0.198 mV/°C; Martz et al. 2010), with a highly linear and stable response to temperature (Takeshita et al. 2014). The ATC is specific to each sensor and is factory set, so the 4–20 mA output of the DL421 module should be able to feed directly to an A/D convertor without requiring further compensation. However, the location of the temperature sensor within the polyphenylene body of the electrode, at some distance (1.3 cm) from the sensing head, means that there is the potential for a lag between the pH measured at the sensing tip and the temperature measured within the housing.

The response of the Durafet to temperature was investigated by Martz et al. (2010) between 5°C and 35°C, who observed a hysteresis effect of up to 0.003 pH during temperature cycling. They attributed the lag to the thermal mass of the Durafet, and potentially to slow re-equilibration of AgCl in the electrode boundary layer (Martz et al. 2010). We observe similar hysteresis effects between −7°C and +12°C, although there was no significant difference between temperature up- and downcycling in our data set. Instead, we observed a relatively constant mean error of 0.02 pH across the entire temperature range when using a simple two-point, low ionic strength calibration. As anticipated, the temperature lags are most significant around the freezing point of the solution (Supporting Information Fig. S3) and likely relate to changes in the actual temperature observed by our monitoring probe—colocated with the Durafet sensing head—and the internal temperature probe. We do not believe that this is a significant barrier to using the Durafet in our target environment, since temperature fluctuations in field settings are likely be minimal (from 0°C to 1°C) and/or gradual, so thermal equilibration of the probe body is expiated. There should also be an external measurement of temperature colocated with the sensing head. This is particularly important in solutions where freeze-thaw occurs, to identify when the solution is fully frozen, and is in accordance with a set of standard operating procedures proposed by Bresnahan Jr et al. (2014).

The remaining uncertainties observed in our laboratory experiments relate to the impact of streaming effects, and of low ionic strength, both of which influence ionic interaction at the surface of the electrode. Even though ISFET sensors are a radically different technology from that of glass electrodes, harnessing an active electronic metal oxide FET, whose oxide coating exchanges protons with a conduction channel when exposed to a solution (Bresnahan Jr et al. 2014), the fundamental physical properties of ionic solutions still control how the sensor measures the pH. When the electrode is inserted into solution, a double layer of charged particles forms at the surface, consisting of those adsorbed to the electrode, and a "cloud" of free ions attracted to the surface charge (Huang et al. 1994). Several authors have proposed the existence of a third layer, which is more mobile and is easily disturbed by stirring (Cheng 2001; Sonnefeld et al. 2001). The presence of this layer and, to some extent, the second layer, causes uncertainty in pH measurements in solutions with variable flow rates, since the charge at the electrode surface varies according to the layer thickness. Faster flows cause disturbance to the layer of charged ions, which operate somewhat like a rubber band (Cheng 2001), flexing as the ions are disturbed and returning to the electrode surface when the solution is still.

Manufacturers of glass electrodes have varying recommendations for stirring, ranging from constant stirring during the measurement to ensuring the solution is static before attempting assessment; a compromise must be met between a sufficiently rapid flow of KCl through the electrode junction and minimizing leakage into the test solution (Davison and Woof 1985). Stirring the solution can reduce the impact of leakage from the glass electrode, but also ensure constant redistribution (or not) of ions attached to the electrode surface. Errors introduced by stirring potential in rainwaters measured by glass electrodes may be > 0.5 pH (Galloway et al. 1979). Our results demonstrate that stirring has a measurable impact on pH measurements by the Durafet sensor (Fig. 3) of up to 0.03 pH, although changing the velocity had little impact at the relatively low speeds we were able to simulate in the laboratory. Many natural waters, including glacial meltwater rivers, are characterized by varying and rapid flow, so in situ measurements must account for these uncertainties. The introduced error is an order of magnitude less than that found for potentiometric glass electrodes commonly deployed in glacial meltwater streams (Ryu and Jacobson 2012; Graly et al. 2017). Therefore, the Durafet still represents a significant improvement on traditional methods for capturing meltwater pH, even in fast flowing waters.

Previous assessment of low ionic strength solutions demonstrated errors of up to 0.31 pH in distilled water and 0.47 in natural water samples (Davison and Woof 1985). Of this error, 0.06 was from liquid junction potential (Busenberg and Plummer 1987), and the remainder results from contamination, incorrect electrode conditioning, drift, and a paucity of ions to deliver the charge effectively to the sensing surface. The charge delivery is the most significant challenge, since this cannot be mitigated by good user practices. We sought to determine the likely impact on ISFET sensors by conducting experiments designed to mimic the performance of the sensors in the field. The Durafet manufacturers (Honeywell) specify that the sensor should not be used in high purity waters < 10 μS cm^{-1}. Our results demonstrate that the sensor can perform adequately ($\pm$ 0.2 pH) in this range; this is below the manufacturer's required accuracy, but is within our requirements (typically $\pm$ 0.5 pH, *see* Bagshaw et al. 2016) and better than that obtained by glass electrodes in low ionic strength solutions (Galloway et al. 1979; Covington et al. 1983; Davison and Woof 1985; Ozeki et al. 1998). The manufacturers and distributors of the Sentron probe do not provide advice for use in low ionic strength solutions, but we demonstrate that the Sentron can achieve at least $\pm$ 0.1 pH at > 50 μS cm^{-1}, and $\pm$ 0.8 pH at < 50 μS cm^{-1}. The errors associated with low ionic strength may be minimized by ensuring that the sensor is calibrated in low ionic strength buffer solutions, and allowing a period of sensor "conditioning" in the target solution (Bresnahan Jr et al. 2014). Attention should also be paid to the calibration procedure, ensuring that low ionic strength buffer solutions are used (Busenberg and Plummer 1987). This can be problematic for higher pH ranges, since these solutions are not as stable as higher ionic strength versions.

Table 1. Maximum uncertainty introduced by each environmental stress tested in the laboratory and field.

Environmental condition	Durafet uncertainty $\pm$ pH	Sentron uncertainty $\pm$ pH
Temperature	0.02	Not tested
Stirring	0.03	Not tested
Drift	0.08	0.17
Low ionic strength	0.20	0.80
Total cumulative error	**0.33**	**0.97**

Much of the work previously presented on methods for automated, high resolution pH measurement is specific to oceanic applications where the required degree of accuracy is far in excess of that required in many freshwater studies. For this reason, many of the technological advances have not yet been applied to the measurement of pH in glacial meltwaters, where ease of use and low power consumption are more pressing concerns (Bagshaw et al. 2016). The ISFET sensors examined here have the advantage of fulfilling these requirements, but also of far superior precision and accuracy to potentiometric glass electrodes. The tests demonstrate that the sensors reviewed can survive freeze-thaw and survive long periods of unattended operation with minimal drift, have a predictable and measureable response to temperature, and that stirring and low ionic strength introduce smaller errors than alternative methods of measurement. We therefore recommend that ISFET sensors are an excellent tool for measuring pH in glacial meltwaters. Table 1 shows the cumulative error introduced by each physical condition for both sensors and demonstrates that the likely uncertainty associated with prolonged use (> 1 month) of the sensors in fast flowing, low temperature, low ionic strength natural waters is $\pm$ 0.33 pH for Durafet, and $\pm$ 0.97 for Sentron. When ionic strengths are > 1 mmol L^{-1}, the total uncertainty decreases to $\pm$ 0.21 pH (Durafet) and $\pm$ 0.57 (Sentron).

Scientific implications of field tests

The field tests showed that the ISFET sensors were able to capture diurnal fluctuations in pH, exhibited at all three field sites. These fluctuations were of the order of $\pm$ 0.3 pH at Kiattut Sermiat (*see* Beaton et al. 2017), $\pm$ 0.8 pH at Leverett Glacier, and $\pm$ 0.2 pH at Bogerbreen. The fluctuations at Kiattut Sermiat and Bogerbreen are within the uncertainty boundaries. However, at Kiattut Sermiat the sensors were maintained daily, with drift testing and temperature simultaneously monitored by an external probe. The pH displayed in Fig. 5B is therefore corrected for drift, and the uncertainties

associated with temperature (0.02) and drift (0.08) can be excluded. The remaining uncertainty is ± 0.2. At Bogerbreen, the Sentron sensor was in situ for just 1 week, therefore the drift error is less significant, and the higher conductivity waters (cf. Greenland melt) mitigate some of the ionic strength error. The diurnal fluctuations at Bogerbreen measured by the Sentron, however, remain within the potential sources of error, so we do not undertake further interpretation.

Clear diurnal variability in pH can be observed in Greenland meltwater records. These diurnal fluctuations are a response to varying discharge and corresponding geochemical conditions at the glacier bed; as temperature and radiation increase during the day, icemelt on the glacier surface is pushed through the glacial drainage system, displacing water stored beneath the glacier. This stored water is characterized by high rock: water contact times and high chemical weathering potential, thus is typically more concentrated than fresh ice melt. The peak in pH is coincident with low flows (Beaton et al. 2017) that have a higher contribution of stored water. This pattern is displayed at both Kiattut Sermiat and Leverett Glacier, from the very beginning of melt season. In the longer time series from Kiattut Sermiat, the key feature is the rise in pH on the 05–06 June, which coincides with the opening up of the subglacial drainage system after the winter (Hawkings et al. 2016; Beaton et al. 2017), commonly referred to as the "Spring Event" (Mair et al. 2003). Fresh ice and snow melt flush out stored water, and the subglacial drainage system reorganizes to transport meltwater rapidly and efficiently to the glacier margins. The chemical weathering regime at Kiattut Sermiat transitions from one dominated by long residence time waters and with hallmarks of silicate weathering coupled to sulfide oxidation, to rapid moving meltwater undergoing carbonate hydrolysis. Hydrolysis reactions drive a pH increase from ~ 8 to ~ 9. Diurnal cycles remain superimposed over this fundamental change in the behavior of the geochemical system, and biological primary production in a proglacial lake upstream of the sampling site may contribute to maintenance of the high pH (Beaton et al. 2017).

pH data at Leverett Glacier are captured from the very first emergence of meltwater in the spring. These waters flowed despite the main meltwater portal appearing frozen (Lamarche-Gagnon et al. 2019) and displayed marked diurnal cycles of up to 0.8 pH. The mean pH declines from ~ 8 to ~ 7.5 over a week, as snow begins to melt and dilute the concentrated waters that have likely been stored over winter. These early season data have never before been captured. Manual sampling for pH at this high temporal resolution is particularly challenging when air temperatures are < 0°C, and automated sampling systems based on glass electrodes typically cannot endure the intense freeze-thaw cycles which characterize the very early melt season (Bagshaw et al. 2016). The data captured give us a valuable insight into the behavior of meltwaters in the very early spring, demonstrating that pH is alkaline in the first melt, despite the influence of snowmelt (Hodson 2006). Thereafter, subglacial waters that have been isolated from the atmosphere begin to emerge and pH increases (Hatton et al. 2019). Notably, the pH at both field sites in the bulk melt season is > 7.5 (Fig. 5; Hatton et al. 2019), indicative of low pCO_2. This contrasts with point measurements assessed by Graly et al. (2017) to imply that subglacial meltwaters can freely exchange with atmospheric gases.

Comments and recommendations

ISFET technology represents a significant advance in the measurement of pH in remote, low temperature environments. The sensors are characterized by minimal drift, stable response, durability, and resistance to many extreme environmental conditions. Our tests have confirmed that two versions of ISFET pH sensors, the Durafet (Honeywell) and Sentron (Campbell Scientific), are suited to deployment in glacial meltwaters, since they can endure freeze-thaw cycling, low temperatures, fast and variable flow, and have low power consumption and good portability. The Sentron probe experiences marked drift (up to 0.17 pH over 2 months), so is not well suited to prolonged deployment without frequent drift tests and corrections. We characterized the response to low ionic strength, and concluded that errors are < 0.2 (Durafet) or < 0.8 (Sentron) pH. Errors can be minimized by using low ionic strength buffers for calibration and preconditioning the electrode prior to use (Bresnahan Jr et al. 2014), but the impact of low ionic strength on accuracy must be considered. An independent temperature probe is recommended to account for thermal lag between the sensor head and temperature sensor within the Durafet. The ISFET sensors allow the measurement of pH in meltwaters at a resolution, precision, and accuracy that has not been possible with alternative methods (glass electrodes or spectrophotometric analysis). While errors remain notable, particularly in comparison to oceanic applications, they represent a significant improvement on other methods employed to date. ISFET sensors are therefore the most reliable technique for measuring pH in remote, fast-changing waters, and have the potential to reveal previously unknown biogeochemical processes in some of the most extreme freshwater systems on Earth.

References

Arrigo, K. R., and others. 2017. Melting glaciers stimulate large summer phytoplankton blooms in southwest Greenland waters. Geophys. Res. Lett. **44**: 6278–6285. doi:10.1002/2017gl073583

Bagshaw, E. A., A. Beaton, J. L. Wadham, M. Mowlem, J. R. Hawkings, and M. Tranter. 2016. Chemical sensors for in situ data collection in the cryosphere. TrAC Trends Analyt. Chem. **82**: 348–357. doi:10.1016/j.trac.2016.06.016

Bamber, J. L., A. J. Tedstone, M. D. King, I. M. Howat, E. M. Enderlin, M. R. v. d. Broeke, and B. Noel. 2018. Land ice

freshwater budget of the Arctic and North Atlantic oceans: 1. Data, methods, and results. J. Geophys. Res. Oceans **123**: 1827–1837. doi:10.1002/2017JC013605

Bartholomew, I., P. Nienow, D. Mair, A. Hubbard, M. A. King, and A. Sole. 2010. Seasonal evolution of subglacial drainage and acceleration in a Greenland outlet glacier. Nat. Geosci. **3**: 408–411. doi:10.1038/ngeo863

Bates, R. G. 1973. Determination of pH: Theory and practice. New York, NY: Wiley.

Beaird, N. L., F. Straneo, and W. Jenkins. 2018. Export of strongly diluted Greenland meltwater from a major Glacial Fjord. Geophys. Res. Lett. **45**: 4163–4170. doi:10.1029/2018gl077000

Beaton, A. D., J. L. Wadham, J. Hawkings, E. A. Bagshaw, G. Lamarche-Gagnon, M. C. Mowlem, and M. Tranter. 2017. High-resolution in situ measurement of nitrate in runoff from the Greenland ice sheet. Environ. Sci. Technol. **51**: 12518–12527. doi:10.1021/acs.est.7b03121

Bergveld, P. 2003. Thirty years of ISFETOLOGY - what happened in the past 30 years and what may happen in the next 30 years. Sens. Actuators B Chem. **88**: 1–20. doi:10.1016/s0925-4005(02)00301-5

Bresnahan, P. J., Jr., T. R. Martz, Y. Takeshita, K. S. Johnson, and M. LaShomb. 2014. Best practices for autonomous measurement of seawater pH with the Honeywell Durafet. Methods Oceanogr. **9**: 44–60. doi:10.1016/j.mio.2014.08.003

Busenberg, E., and L. N. Plummer. 1987. pH measurement of low-conductivity waters, p. 1–22. US Geological Survey Water-Resources Investigations Report 87. doi:10.3133/wri874060

Cheng, K. L. 2001. Counterion triple layer in solid/solution interface: Stirring and temperature effects on pH measurements. J. Colloid Interface Sci. **239**: 385–390. doi:10.1006/jcis.2001.7580

Clayton, T. D., and R. H. Byrne. 1993. Spectrophotometric seawater pH measurements - total hydrogen-ion concentration scale calibration of M-cresol purple and at-sea results. Deep-Sea Res. Part I Oceanogr. Res. Pap. **40**: 2115–2129. doi:10.1016/0967-0637(93)90048-8

Covington, A. K., P. D. Whalley, and W. Davison. 1983. Procedures for the measurement of pH in low ionic strength solutions including freshwater. Analyst **108**: 1528–1532. doi:10.1039/AN9830801528

Cowton, T., P. Nienow, I. Bartholomew, A. Sole, and D. Mair. 2012. Rapid erosion beneath the Greenland ice sheet. Geology **40**: 343–346. doi:10.1130/g32687.1

Davison, W., and C. Woof. 1985. Performance tests for the measurement of pH with glass electrodes in low ionic strength solutions including natural waters. Anal. Chem. **57**: 2567–2570. doi:10.1021/ac00290a031

Dickson, A. G., C. L. Sabine, and J. R. Christian. 2007. SOP 6b: Determination of the pH of seawater using the indicator dye m-cresol purple, p. 191. *In* A. G. Dickson, C. L. Sabine, and J. R. Christian [eds.], Guide to best practices for ocean CO_2 measurements. PICES Special Publication 3. Sidney, Canada: North Pacific Marine Science Organization.

Fransson, A., M. Chierici, D. Nomura, M. A. Granskog, S. Kristiansen, T. Martma, and G. Nehrke. 2015. Effect of glacial drainage water on the CO_2 system and ocean acidification state in an Arctic tidewater-glacier fjord during two contrasting years. J. Geophys. Res. Oceans **120**: 2413–2429. doi:10.1002/2014jc010320

Galloway, J. N., B. J. Cosby, and G. E. Likens. 1979. Acid precipitation: Measurement of pH and acidity. Limnol. Oceanogr. **24**: 1161–1165. doi:10.4319/lo.1979.24.6.1161

Gonski, S., W.-J. Cai, W. J. Ullman, A. Joesoef, C. Main, D. Tye Pettay, and T. R. Martz. 2017. Assessment of the suitability of Durafet-based sensors for pH measurement in dynamic estuarine environments. Estuar. Coast. Shelf Sci. **200**: 152–168. doi:10.1016/j.ecss.2017.10.020

Graly, J. A., J. I. Drever, and N. F. Humphrey. 2017. Calculating the balance between atmospheric CO_2 drawdown and organic carbon oxidation in subglacial hydrochemical systems. Global Biogeochem. Cycles **31**: 709–727. doi:10.1002/2016GB005425

Hatton, J. E., K. R. Hendry, J. R. Hawkings, J. L. Wadham, T. J. Kohler, M. Stibal, A. D. Beaton, E. A. Bagshaw, and J. Telling. 2019. Investigation of subglacial weathering under the Greenland Ice Sheet using silicon isotopes. Geochim. Cosmochim. Acta **247**: 191–206. doi:10.1016/j.gca.2018.12.033

Hawkings, J., and others. 2016. The Greenland Ice Sheet as a hot spot of phosphorus weathering and export in the Arctic. Global Biogeochem. Cycles **30**: 191–210. doi:10.1002/2015gb005237

Hawkings, J. R., and others. 2015. The effect of warming climate on nutrient and solute export from the Greenland Ice Sheet. Geochem. Perspect. Lett. **1**: 94–104. doi:10.7185/geochemlet.1510

Hendry, K. R., and others. 2019. The biogeochemical impact of glacial meltwater from Southwest Greenland. Prog. Oceanogr. **176**: 102126. doi:10.1016/j.pocean.2019.102126

Hodson, A. 2006. Biogeochemistry of snowmelt in an Antarctic glacial ecosystem. Water Resour. Res. **42**: W11406. doi:10.1029/2005wr004311

Hofmann, G. E., and others. 2011. High-frequency dynamics of ocean pH: A multi-ecosystem comparison. PLoS One **6**: e28983. doi:10.1371/journal.pone.0028983

Hood, E., T. J. Battin, J. Fellman, S. O'Neel, and R. G. M. Spencer. 2015. Storage and release of organic carbon from glaciers and ice sheets. Nat. Geosci. **8**: 91–96. doi:10.1038/ngeo2331

Hood, E., J. Fellman, R. G. M. Spencer, P. J. Hernes, R. Edwards, D. D'Amore, and D. Scott. 2009. Glaciers as a source of ancient and labile organic matter to the marine environment. Nature **462**: 1044–1047. doi:10.1038/nature08580

Hopwood, M. J., D. Carroll, T. J. Browning, L. Meire, J. Mortensen, S. Krisch, and E. P. Achterberg. 2018. Non-linear response of summertime marine productivity to increased meltwater discharge around Greenland. Nat. Commun. **9**: 3256. doi:10.1038/s41467-018-05488-8

Hopwood, M. J., and others. 2020. How does glacier discharge affect marine biogeochemistry and primary production in the Arctic? Cryosphere **14**: 1347–1383. doi:10.5194/tc-14-1347-2020

Huang, C.-I., H. Huang, and K. L. Cheng. 1994. Effect of stirring on pH measurements, p. 227–240. *In* T. Yen, R. Gilbert, and J. Fendler [eds.], Advances in the applications of membrane-mimetic chemistry. Springer.

Johnson, K. S., H. W. Jannasch, L. J. Coletti, V. A. Elrod, T. R. Martz, Y. Takeshita, R. J. Carlson, and J. G. Connery. 2016. Deep-Sea DuraFET: A Pressure Tolerant pH Sensor Designed for Global Sensor Networks. Anal. Chem. **88**: 3249–3256. doi:10.1021/acs.analchem.5b04653

Kellerman, A. M., and others. 2020. Glacier outflow dissolved organic matter as a window into seasonally changing carbon sources: Leverett Glacier, Greenland. J. Geophys. Res. Biogeosci. **125**: e2019JG005161. doi:10.1029/2019jg005161

Knudsen, N. T., J. C. Yde, and G. Gasser. 2007. Suspended sediment transport in glacial meltwater during the initial quiescent phase after a major surge event at Kuannersuit Glacier, Greenland. Geogr. Tidsskr. **107**: 1–7. doi:10.1080/00167223.2007.10801370

Lai, C.-Z., and others. 2017. Spectrophotometric measurement of freshwater pH with purified meta-cresol purple and phenol red. Limnol. Oceanogr.: Methods **15**: 903–903. doi:10.1002/lom3.10210

Lamarche-Gagnon, G., J. L. Wadham, B. Sherwood Lollar, S. Arndt, P. Fietzek, G. Lacrampe-Couloume, A. Beaton, A. Tedstone, J. Telling, E. A. Bagshaw, J. Hawkings, T. Kohler, J. Zarsky, M. Mowlem, A. Anesio, and M. Stibal. 2019. Greenland melt drives continuous export of methane from the ice-sheet bed. Nature. **565**: 73–77. doi:10.1038/s41586-018-0800-0

Liu, X. W., M. C. Patsavas, and R. H. Byrne. 2011. Purification and characterization of meta-cresol purple for spectrophotometric seawater pH measurements. Environ. Sci. Technol. **45**: 4862–4868. doi:10.1021/es200665d

Mair, D., I. Willis, U. H. Fischer, B. Hubbard, P. Nienow, and A. Hubbard. 2003. Hydrological controls on patterns of surface, internal and basal motion during three "spring events": Haut Glacier D'arolla, Switzerland. J. Glaciol. **49**: 555–567. doi:10.3189/172756503781830467

Martz, T. R., J. G. Connery, and K. S. Johnson. 2010. Testing the Honeywell Durafet® for seawater pH applications. Limnol. Oceanogr.: Methods **8**: 172–184. doi:10.4319/lom.2010.8.172

Matson, P. G., T. R. Martz, and G. E. Hofmann. 2011. High-frequency observations of pH under Antarctic sea ice in the southern Ross Sea. Antarct. Sci. **23**: 607–613. doi:10.1017/S0954102011000551

Matson, P. G., L. Washburn, T. R. Martz, and G. E. Hofmann. 2014. Abiotic versus biotic drivers of ocean pH variation under fast sea ice in Mcmurdo Sound, Antarctica. PLoS One **9**: e107239. doi:10.1371/journal.pone.0107239

McLaughlin, K., and others. 2017. An evaluation of ISFET sensors for coastal pH monitoring applications. Reg. Stud. Mar. Sci. **12**: 11–18. doi:10.1016/j.rsma.2017.02.008

Metcalf, R. C. 1984. Field pH determinations in glacial melt waters. J. Glaciol. **30**: 106–111. doi:10.3189/S0022143000008546

Ozeki, T., Y. Tsubosaka, S. Nakayama, N. Ogawa, and T. Kimoto. 1998. Study of errors in determination of hydrogen ion concentrations in rainwater samples using glass electrode method. Anal. Sci. **14**: 749–756. doi:10.2116/analsci.14.749

Patsavas, M. C., R. H. Byrne, and X. Liu. 2013. Purification of meta-cresol purple and cresol red by flash chromatography: Procedures for ensuring accurate spectrophotometric seawater pH measurements. Mar. Chem. **150**: 19–24. doi:10.1016/j.marchem.2013.01.004

Raiswell, R., J. Hawkings, A. Eisenousy, R. Death, M. Tranter, and J. Wadham. 2018. Iron in glacial systems: Speciation, reactivity, freezing behavior, and alteration during transport. Front. Earth Sci. **6**: 222. doi:10.3389/feart.2018.00222

Rérolle, V., D. Ruiz-Pino, M. Rafizadeh, S. Loucaides, S. Papadimitriou, M. Mowlem, and J. Chen. 2016. Measuring pH in the Arctic Ocean: Colorimetric method or SeaFET? Methods Oceanogr. **17**: 32–49. doi:10.1016/j.mio.2016.05.006

Rerolle, V. M. C., C. F. A. Floquet, M. C. Mowlem, R. Bellerby, D. P. Connelly, and E. P. Achterberg. 2012. Seawater-pH measurements for ocean-acidification observations. TrAC Trends Analyt. Chem. **40**: 146–157. doi:10.1016/j.trac.2012.07.016

Ryu, J.-S., and A. D. Jacobson. 2012. CO_2 evasion from the Greenland Ice Sheet: A new carbon-climate feedback. Chem. Geol. **320-321**: 80–95. doi:10.1016/j.chemgeo.2012.05.024

Sonnefeld, J., M. Lobbus, and W. Vogelsberger. 2001. Determination of electric double layer parameters for spherical silica particles under application of the triple layer model using surface charge density data and results of electrokinetic sonic amplitude measurements. Colloids Surf A Physicochem. Eng. Asp. **195**: 215–225. doi:10.1016/s0927-7757(01)00845-7

St. Pierre, K. A., V. L. St. Louis, S. L. Schiff, I. Lehnherr, P. G. Dainard, A. S. Gardner, P. J. K. Aukes, and M. J. Sharp. 2019. Proglacial freshwaters are significant and previously unrecognized sinks of atmospheric CO_2. Proc. Natl. Acad. Sci. USA **116**: 17690–17695. doi:10.1073/pnas.1904241116

Takeshita, Y., T. R. Martz, K. S. Johnson, and A. G. Dickson. 2014. Characterization of an ion sensitive field effect

transistor and chloride ion selective electrodes for pH measurements in seawater. Anal. Chem. **86**: 11189–11195. doi: 10.1021/ac502631z

Tranter, M. 2003. Geochemical weathering in glacial and proglacial environments, p. 189–205.*In* J. I. Drever [ed.], Treatise on geochemistry: Surface and ground water, weathering and soils, v. **5**. Elsevier.

Tranter, M., A. G. Fountain, C. H. Fritsen, W. B. Lyons, J. C. Priscu, P. J. Statham, and K. A. Welch. 2004. Extreme hydrochemical conditions in natural microcosms entombed within Antarctic ice. Hydrol. Process. **18**: 379–387. doi:10.1002/hyp.5217.

Wadham, J. L., J. R. Hawkings, L. Tarasov, L. J. Gregoire, R. G. M. Spencer, M. Gutjahr, A. Ridgwell, and K. E. Kohfeld. 2019. Ice sheets matter for the global carbon cycle. Nat. Commun. **10**: 3567. doi:10.1038/s41467-019-11394-4

Acknowledgments

This work was funded by NERC DELVE (NE/I008845/1), with fieldwork supported by an enthusiastic team of assistants in Greenland and Svalbard. Particular thanks are extended to Jon Telling, Lisa Mol, Blue Ice Greenland, Kangerlussuaq International Science Support Centre and UNIS Svalbard. Henrik Sass provided invaluable assistance with purification of the mCP indicator, and discussion with Socratis Loucaides gave helpful advice on testing methods. Three reviewers are thanked for their constructive suggestions to improve the text.

Conflict of Interest

None declared.

Submitted 20 July 2020
Revised 14 October 2020
Accepted 30 December 2020

Associate editor: Christian Fritsen